Discover Oncology

Research

An integrative analysis combining bioinformatics, network pharmacology and experimental methods identified key genes of EGCG targets in Nasopharyngeal Carcinoma

Yuhang Yang[1] · Wenqi Luo[2] · Zhang Feng[1] · Xiaoyu Chen[2] · Jinqing Li[1] · Long Zuo[1] · Meijiao Duan[1] · Xiaosong He[1] · Wenhua Wang[1] · Feng He[1] · Fangxian Liu[1]

Received: 17 November 2024 / Accepted: 10 April 2025
Published online: 12 May 2025

Abstract

Background Epigallocatechin gallate (EGCG), a frequently studied catechin in green tea, has been shown to be involved in the antiproliferation and apoptosis of human Nasopharyngeal carcinoma (NPC) cells. However, the pharmacological targets and mechanism by which EGCG can combat NPC patients remain to be studied in detail.

Methods Network pharmacology and bioinformatics were employed to investigate the molecular mechanisms underlying EGCG's therapeutic effects on NPC, with an emphasis on developing a prognostic risk model and identifying potential therapeutic targets.

Results A novel prognostic risk model was developed using univariate Cox regression, LASSO regression and multivariable Cox regression analyses, incorporating six genes to stratify patients into low- and highrisk groups. Kaplan–Meier analysis demonstrated significantly shorter progression-free survival in the high-risk group. The model's accuracy was further validated using time-dependent Receiver Operating Characteristic (ROC) curves. ESTIMATE analysis revealed significantly higher immune, stromal and overall ESTIMATE scores in the low-risk group compared to the high-risk group. Immune profiling indicated significant differences in five immune cell subtypes (memory B cells, regulatory T cells (Tregs), gamma delta T cells, activated NK cells and activated dendritic cells) between the two risk groups. Additionally, the low-risk group showed greater sensitivity to conventional chemotherapeutic agents. Immunohistochemistry and molecular docking analyses identified CYCS and MYL12B as promising targets for EGCG treatment.

Conclusion This study utilised network pharmacology and bioinformatics to identify shared genes between EGCG and NPC, aiming to elucidate the molecular mechanisms through which EGCG inhibits NPC and to develop a prognostic model for assessing patient outcomes. The findings provide potential insights for the development of anti-NPC therapies and their clinical applications.

Keywords EGCG · Nasopharyngeal carcinoma · Network pharmacology · Bioinformatics · Prognostic signature · Tumor microenvironment

Yuhang Yang and Wenqi Luo contributed equally to this work.

Supplementary Information The online version contains supplementary material available at https://doi.org/10.1007/s12672-025-02365-x.

✉ Feng He, hefeng19880604@outlook.com; ✉ Fangxian Liu, lfx9911008@163.com | [1]Department of Otolaryngology Head and Neck Surgery, Affiliated Hospital of Guilin Medical University, Guilin 541001, China. [2]Department of Pathology, Guangxi Medical University Cancer Hospital, Nanning 530021, China.

Abbreviations

AUC	Area under the curve
BP	Biological processes
DEGs	Differentially expressed genes
IHC	Immunohistochemistry
HNSCC	Head and neck squamous cell carcinoma
GSEA	Gene Set Enrichment Analysis
GO	Gene ontology
PFS	Progression-free survival
KEGG	Kyoto Encyclopedia of Genes and Genomes
K–M	Kaplan–Meier
LASSO	Least absolute shrinkage and selection operator
CC	Cellular components
MF	Molecular functions
OS	Overall survival
ROC	Receiver operating characteristic
EGCG	Epigallocatechin gallate
TME	Tumor microenvironment
TCGA	The cancer Genome Atlas

1 Introduction

Nasopharyngeal carcinoma (NPC) exhibits a distinct geographic distribution, with particularly high incidence rates in East and Southeast Asia [1]. Factors such as variations in dietary habits, lifestyles and environmental exposures contribute to the regional differences in NPC incidence. Additionally, ethnicity-related genetic variations and the presence of the Epstein-Barr virus (EBV) are significant contributors to NPC pathogenesis [2]. However, the molecular mechanisms underlying NPC remain poorly understood, and few targeted therapies have been developed for its treatment. Cisplatin and paclitaxel, as first-line chemotherapeutic agents, have demonstrated efficacy in improving NPC treatment outcomes. However, high doses of these cytotoxic drugs often lead to severe side effects and the development of multidrug resistance, ultimately resulting in treatment failure [3]. Therefore, identifying chemotherapeutic agents with high efficacy and lower toxicity is crucial for enhancing clinical outcomes and improving patient survival.

Natural products have historically played an important role in pharmacotherapy, particularly in cancer and infectious disease treatment [4, 5]. EGCG, a polyphenol derived from green tea, has been shown to possess various health benefits, including anti-tumour, antioxidant, anti-inflammatory, cardiovascular and neuroprotective effects [6, 7]. Recent studies suggest that EGCG inhibits NPC cell proliferation and enhances their sensitivity to radiotherapy, indicating its potential as a therapeutic agent for NPC [7, 8]. However, the specific molecular targets of EGCG in NPC cells remain unclear, and further investigation into its regulatory mechanisms is essential for identifying novel therapeutic targets. In recent years, gene signatures have gained prominence in cancer prognosis. Numerous studies have employed bioinformatics approaches to identify genes involved in critical biological pathways [9–12], highlighting their importance not only for cancer diagnosis but also for the development of robust prognostic models.

In this study, we employed high-throughput methods to comprehensively analyse and identify potential target genes of EGCG. We also identified key gene clusters associated with patient prognosis, developed diagnostic and prognostic models for NPC, explored their relationship with chemotherapy response and tumour immune infiltration, and validated the expression of selected targets. Our findings may contribute to improved early diagnosis of NPC and offer valuable insights into patient outcomes.

2 Results

2.1 Identifcation of DEGs related to potential targets of EGCG from HK1 NPC cell lines and functional enrichment analysis

The workflow of this study is outlined in Fig. 1. To identify potential EGCG targets, we utilised GeneCards, TCMSP, TargetNet and SwissTargetPrediction databases, yielding 588, 140, 114 and 100 targets, respectively. After removing duplicates,

we compiled 734 unique EGCG targets for differential expression analysis in HK1 NPC cell lines (Supplementary Table 1). Applying a threshold of $p < 0.05$, we identified 198 DEGs, with 88 upregulated and 110 downregulated genes. Detailed information on these DEGs is provided in Supplementary Table 2. A volcano plot depicting the DEGs is shown in Fig. 2A, while a heatmap in Fig. 2B presents the top 50 upregulated and downregulated DEGs. Subsequent KEGG pathway analysis revealed significant enrichment in pathways such as lipid and atherosclerosis, hepatitis B, measles, non-alcoholic fatty liver disease, apoptosis, Kaposi sarcoma-associated herpesvirus infection, the neurotrophin signalling pathway and the IL-17 signalling pathway (Fig. 2C). Gene Ontology (GO) analysis indicated that DEGs were primarily involved in biological processes (BP) such as response to oxidative stress, cellular response to chemical stress and nutrient levels. The DEGs were also associated with cellular components (CC) including focal adhesion, cell-substrate junctions and secretory granule lumens. Molecular functions (MF) predominantly involved RNA polymerase II-specific DNA-binding transcription factor binding, DNA-binding transcription factor binding and protein phosphatase binding(Fig. 2D).

2.2 Screening for prognostic markers and establishment of a prognostic model for patients with NPC

To identify prognostic markers for NPC, Cox and LASSO regression analyses were performed on the 113 DEGs identified in the GSE102349 dataset. Initially, univariate

Cox regression analysis revealed that 31 DEGs were significantly associated with PFS in NPC patients (Fig. 3A). To ensure the stability and clinical applicability of these genes, LASSO Cox regression was applied, further narrowing the list to 10 genes (Fig. 3B and C). Finally, multivariate Cox regression identified six-genes (SNCG, FOXO3, MYL12B, PTGS1, CDKN2 A, and CYCS)that were used to construct a prognostic model for PFS (Fig. 3D)(Supplementary Table 3).

A risk score was calculated based on the Cox coefficient for each gene, using the following formula: Risk score =—0.5342 × expression level of SNCG + 0.9567 × expres-sion level of FOXO3—1.3144 × expression level of MYL12B—0.7801 × expression level of PTGS1—0.5497 × expression level of CDKN2 A + 1.8118 × expression level of CYCS. Subsequently, Patients were stratified into high-risk and low-risk groups based on the median risk score. Kaplan–Meier analysis was then employed to evaluate the PFS between the two groups. The results demonstrated that the high-risk group had a significantly shorter PFS compared to the low-risk group (Fig. 4A, B). The pre-dictive performance of the risk score was further supported by area under the curve (AUC) values of 0.856, 0.867 and 0.942 at one, two and three years, respectively (Fig. 4C). Furthermore, we utilized the cut-off value of the median risk score derived from the GSE102349 cohorts to establish a boundary between the high-risk and low-risk groups within the HNSCC cohort, thereby validating its reliability and reproducibility (Supplementary Table 4). Kaplan–Meier analysis confirmed that HNSCC patients with high-risk scores had worse overall survival (Fig. 4D, E). Time-dependent ROC curve analysis indicated that the AUC values for 1-year, 2-year and 3-year survival were 0.594, 0.625 and 0.628, respectively (Fig. 4F).

2.3 Relationship between the six-gene prognostic risk model and the immune microenvironment

The CIBERSORT algorithm was applied to the GSE102349 dataset to explore the relationship between the six-gene prognostic risk model and immune cell infiltration in NPC. Figure 5A presents the proportions of 22 immune cell types across the samples. Significant differences were observed in five specific immune cell subtypes between high-risk and low-risk groups: memory B cells, regulatory T cells (Tregs), gamma delta T cells, activated NK cells and activated dendritic cells. Specifically, memory B cells, Tregs and gamma delta T cells were found to be significantly more abundant in the low-risk group, while activated NK cells and activated dendritic cells showed higher infiltration densities in the high-risk group (Fig. 5B). Further comparison of stromal, immune and ESTIMATE scores between the two groups revealed that all three scores were significantly higher in the low-risk group ($p < 0.001$) (Fig. 5C). These results sug-gest substantial differences in the immune microenvironment, indicating that high-risk patients may experience more pronounced immune dysfunction and a greater degree of immunosuppression compared to low-risk patients. In addition, the expression of immune checkpoint genes was analysed between high- and low-risk groups. As shown in Fig. 5D, the low-risk group exhibited higher expression of several immune checkpoint genes, including BTLA, CTLA-4 and PDCD1. These findings suggest that the six-gene prognostic risk model may serve as a valuable tool for assessing NPC immunotherapy responses and guiding clinical decision-making.

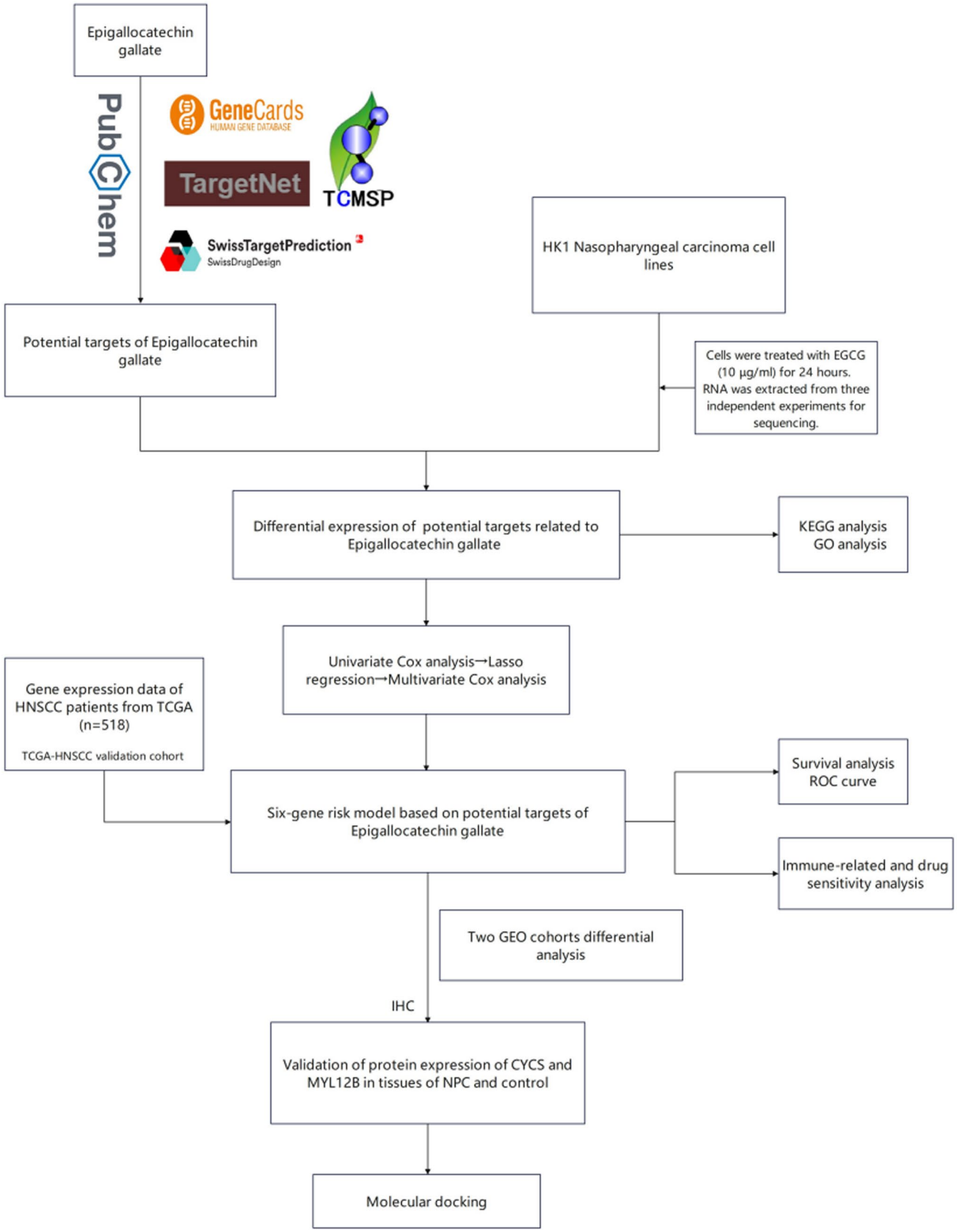

Fig. 1 Complete workflow of our research. "n" denotes sample size. "$p < 0.05$" denotes the statistically significant threshold

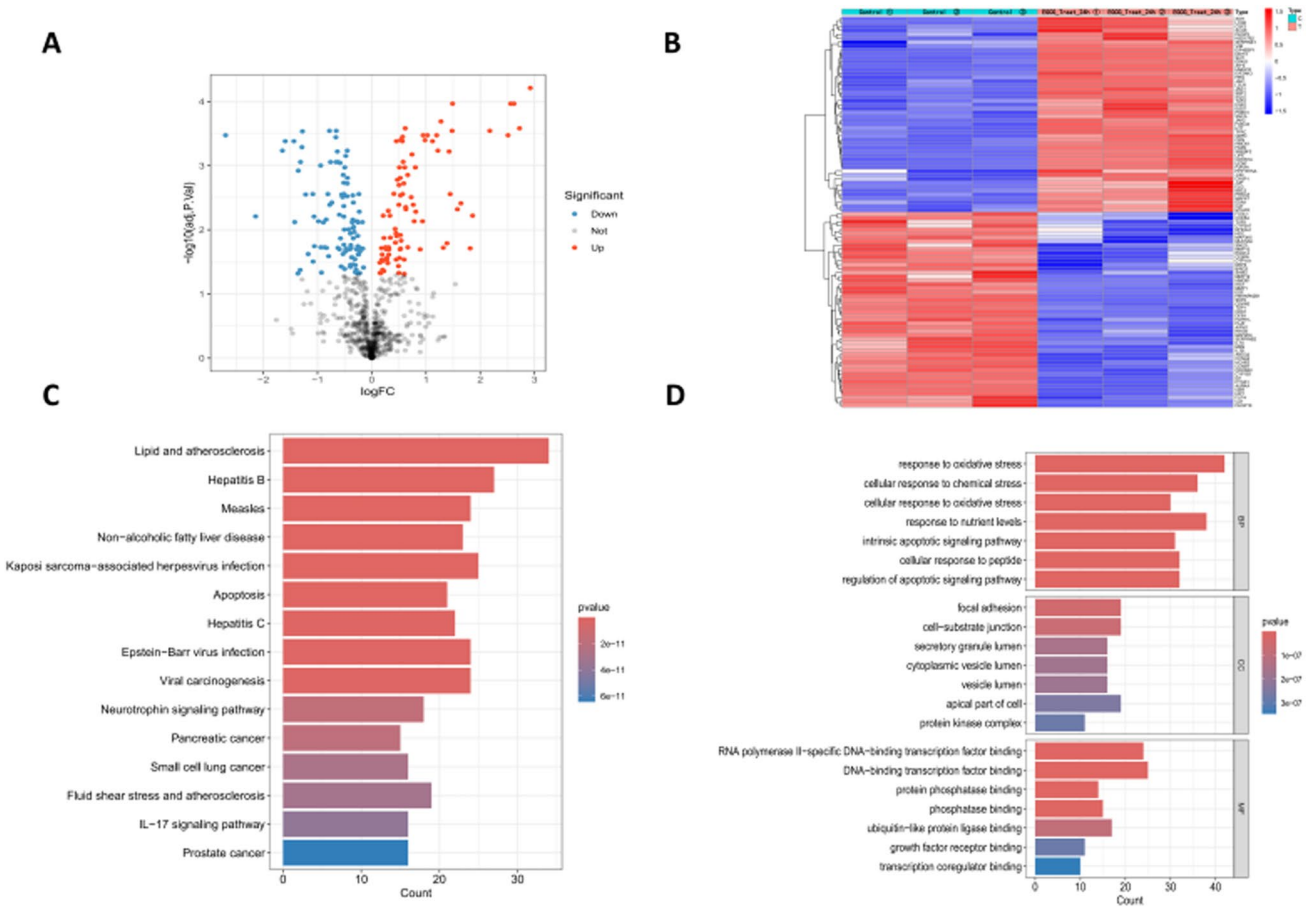

Fig. 2 Identifcation of DEGs related to potential targets of EGCG. **A** Volcano plot of the DEGs. **B** Heat map of the DEGs. **C** Kyoto Encyclopedia of Genes and Genomes (KEGG) analysis of the DEGs. **D** Gene Ontology (GO) analysis of the DEGs

2.4 Comparisons of drug sensitivity

To further investigate the clinical utility of the six-gene prognostic risk model in NPC treatment, we assessed the therapeutic efficacy of frequently prescribed chemotherapeutic medications in different risk groups. According to the findings, low-risk group were more responsive to ATRA, Dasatinib, Gefitinib, Metformin, and Sunitinib, while less sensitive to Docetaxel (Fig. 6A–F).

2.5 Verification of protein expression of CYCS and MYL12B in clinical samples by using immunohistochemistry

To validate the gene expression levels from the risk model, we utilised the GSE53819 and GSE12452 datasets to compare normal and NPC samples (Figure S1). The results showed that CYCS expression was significantly elevated in NPC samples compared to normal controls ($P < 0.001$) (Fig. 7A), whereas MYL12B expression was significantly downregulated in NPC samples ($P < 0.05$) (Fig. 7C). Based on these findings and previous regression analyses, CYCS appears to be a poor prognostic biomarker for NPC, while MYL12B may serve as a protective factor. Additionally, in the differential expression volcano plot, CYCS was downregulated and MYL12B was upregulated in NPC cell lines, in contrast to the results from transcriptome differential analysis (Fig. 7B). This discrepancy suggests that EGCG might downregulate CYCS and upregulate MYL12B, identifying both genes as potential targets for EGCG treatment.

To confirm the protein expression levels of CYCS and MYL12B, we performed immunohistochemical analysis on tumour tissues from 36 NPC cases, adjacent tissues, and 24 normal nasopharyngeal samples. The results demonstrated that CYCS protein expression was significantly higher in NPC tissues compared to normal nasopharyn-geal epithelial tissues (Fig. 8A,

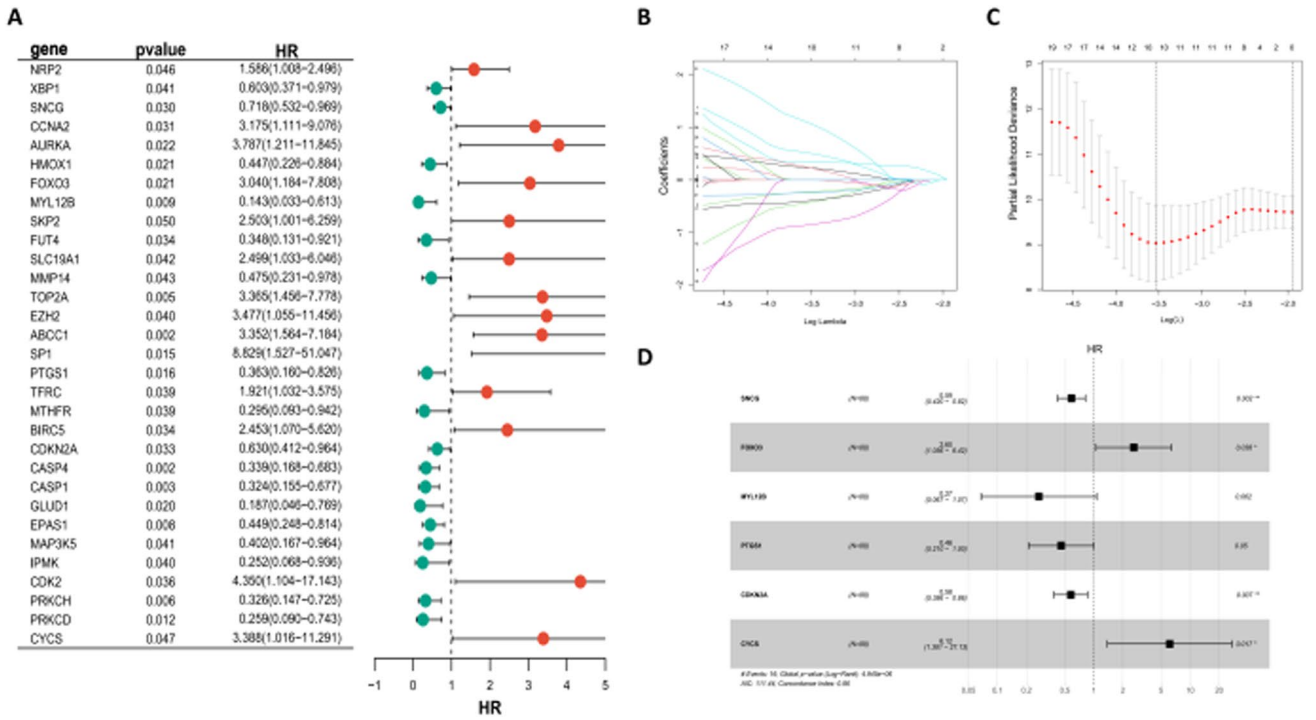

Fig. 3 Screening for prognostic markers in the GSE102349 data set. **A** Univariate Cox regression analysis revealed that the 31 DEGs significantly correlated with NPC prognosis. **B** The LASSO coefficient profile of EGCG potential targets. **C** The tenfold cross-validation for variable selection in the LASSO model. **D** Multivariate Cox regression analysis showed 6 independent prognostic genes

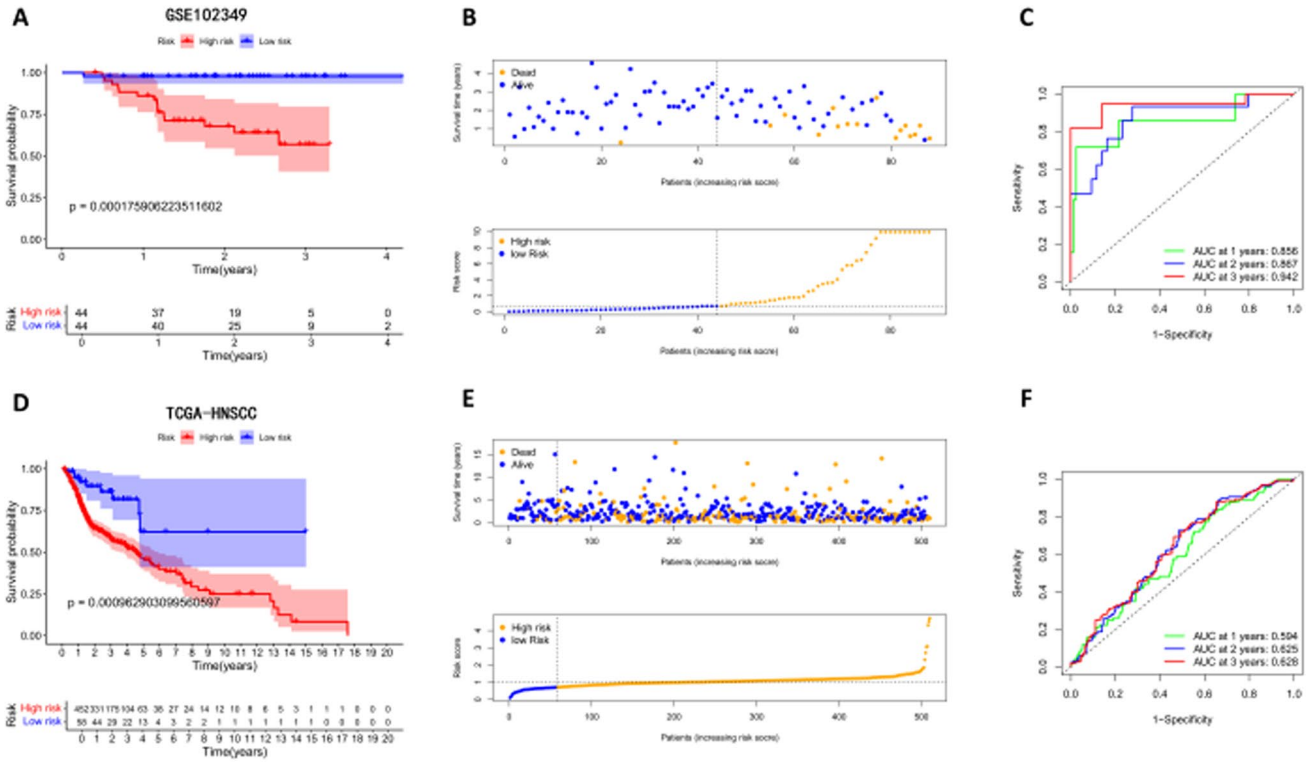

Fig. 4 Construction and validation of prognostic model. **A** Kaplan–Meier survival curves of the PFS of high-risk and low-risk patients in the GSE102349 cohort. **B** Survival status scatter plots and risk score distribution in the GSE102349 cohort. **C** Time-dependent receiver operating characteristic (ROC) curve analysis in GSE102349 cohort. **D** Kaplan–Meier survival curves of the OS of high-risk and low-risk patients in the TCGA-HNSCC cohort. **E** Survival status scatter plots and risk score distribution in the TCGA-HNSCC cohort. **F** Time-dependent receiver operating characteristic (ROC) curve analysis in the TCGA-HNSCC cohort

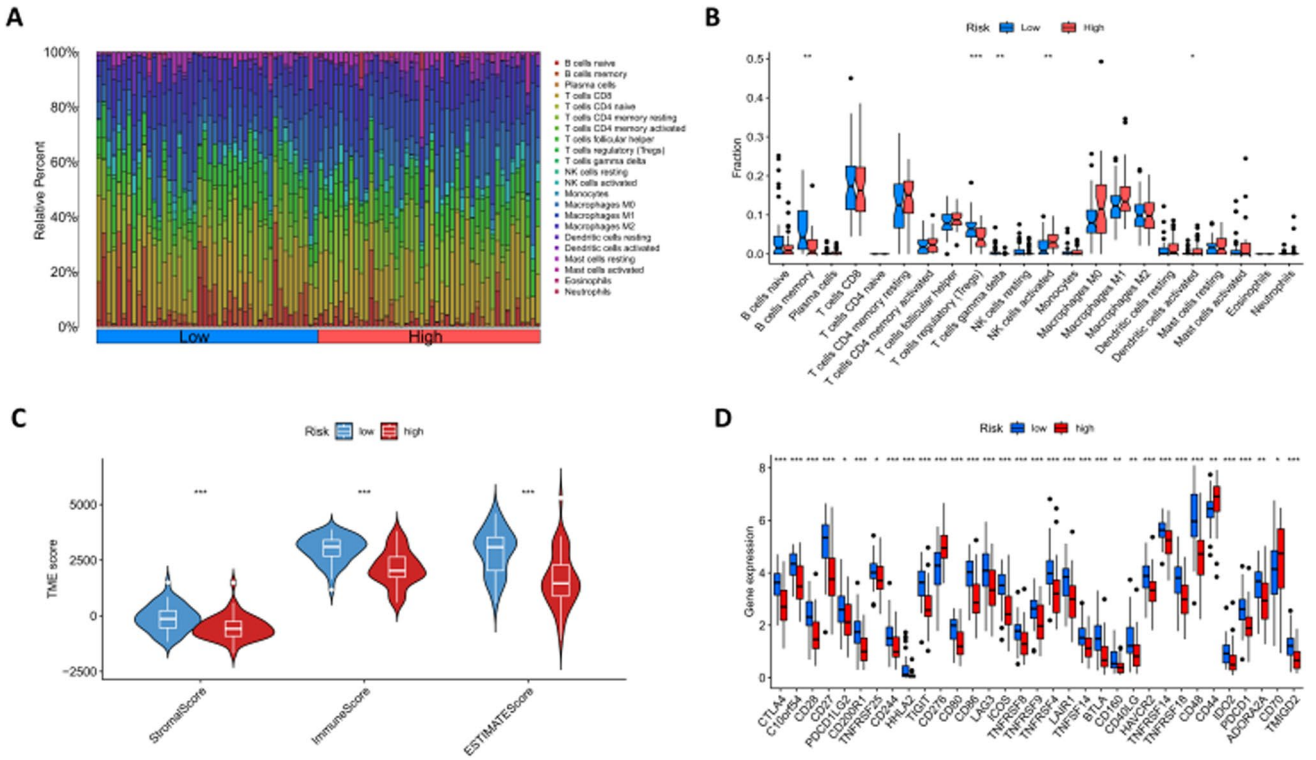

Fig. 5 Immune landscape of the six-gene prognostic risk model. **A** Visualization of immune cell infiltration by the CIBERSORT algorithm. **B** Boxplots illustrating immune cell infiltration between the two subgroups by the ssGSEA algorithm. **C** Tumor microenvironment analysis: Violin plot comparing stromal scores, immune scores and ESTIMATE scores. **D** Boxplots depict different expression levels of immune checkpoint genes between the high-risk and low-risk groups

B). Conversely, MYL12B protein levels were lower in NPC tissues compared to normal samples (Fig. 8D, E), consistent with previous transcriptome differential analyses. ROC curve analysis of the immunohistochemistry staining scores for CYCS and MYL12B (Fig. 8C, F) further validated their diagnostic potential in NPC.

2.6 Molecular docking results

Molecular docking studies were conducted using Autodock Tools v.1.5.7 and AutodockVina software to assess the interactions between EGCG and key target proteins (CYCS and MYL12B). The aim was to evaluate the binding affinities of EGCG with these targets and verify previous analytical results. Binding energy values below 0 kcal/mol suggest a binding activity, while energies lower than 5.0 kcal/mol indicate strong affinity. Although only the computed structural model for MYL12B was available, no experimental data exist to validate its accuracy. The docking results of the binding energies between EGCG and the two receptor proteins are shown in Table 1. According to the results of our molecular docking, the molecular docking of EGCG with key target receptor proteins was plotted, as illustrated in Fig. 9, the binding energies of EGCG with both CYCS and MYL12B were less than 5.0 kcal/mol, indicating strong binding affinities. These results underscore the potential involvement of these targets in mediating the anti-NPC effects of EGCG.

3 Materials and methods

3.1 Acquisition of EGCG potential targets

Pharmacological targets of EGCG were identified using several online databases, including the Traditional Chinese Medicine Systems Pharmacology Database and Analysis Platform (TCMSP), SwissTargetPrediction, TargetNet and GeneCards [13, 14]. In GeneCards (https://www.genecards.org), EGCG targets were searched using the keyword"Epigallocatechin gallate." The canonical SMILES and chemical structure of EGCG were obtained from

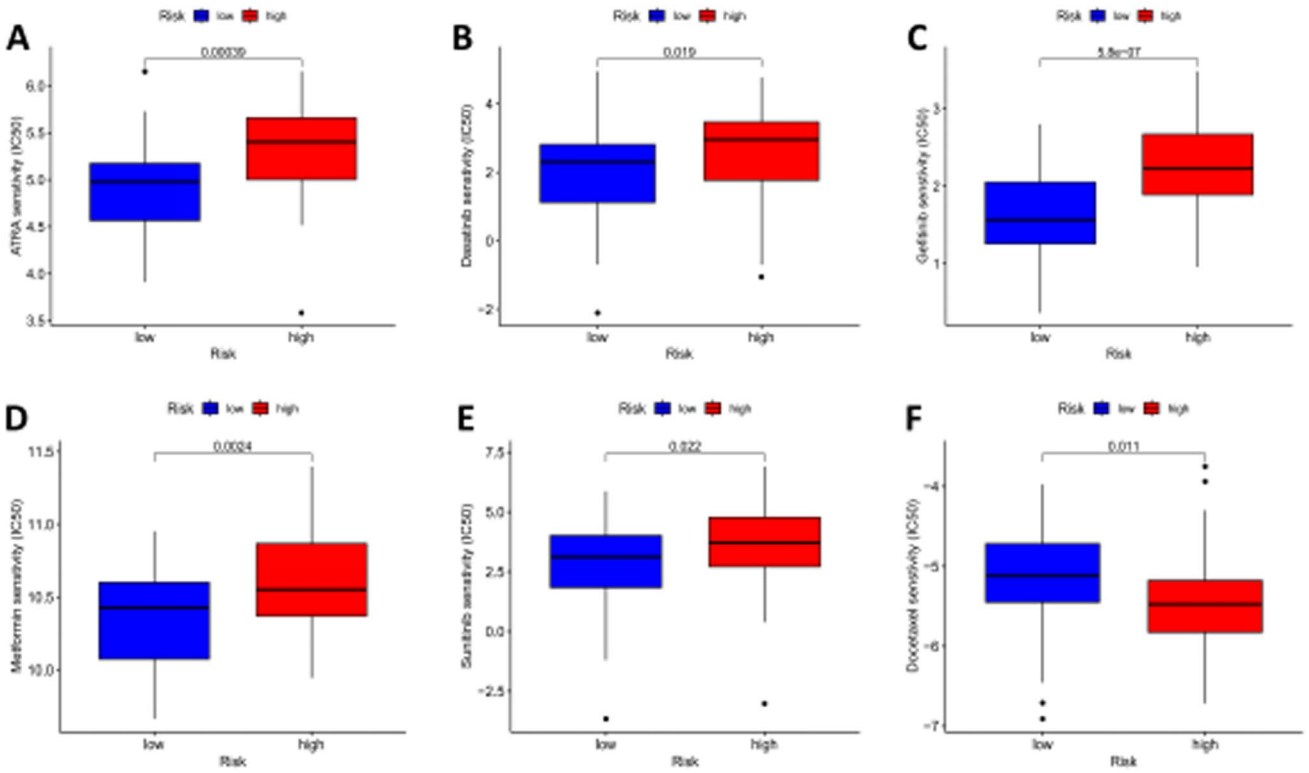

Fig. 6 Comparison of treatment drugs senstivity between high- and low-risk groups. **A** IC50 of ATRA in high and low risk groups. **B** IC50 of Dasatinib in high and low risk groups. **C** IC50 of Gefitinib in high and low risk groups. **D** IC50 of Metformin in high and low risk groups. **E** IC50 of Sunitinib in high and low risk groups. **F** IC50 of Docetaxel in high and low risk groups

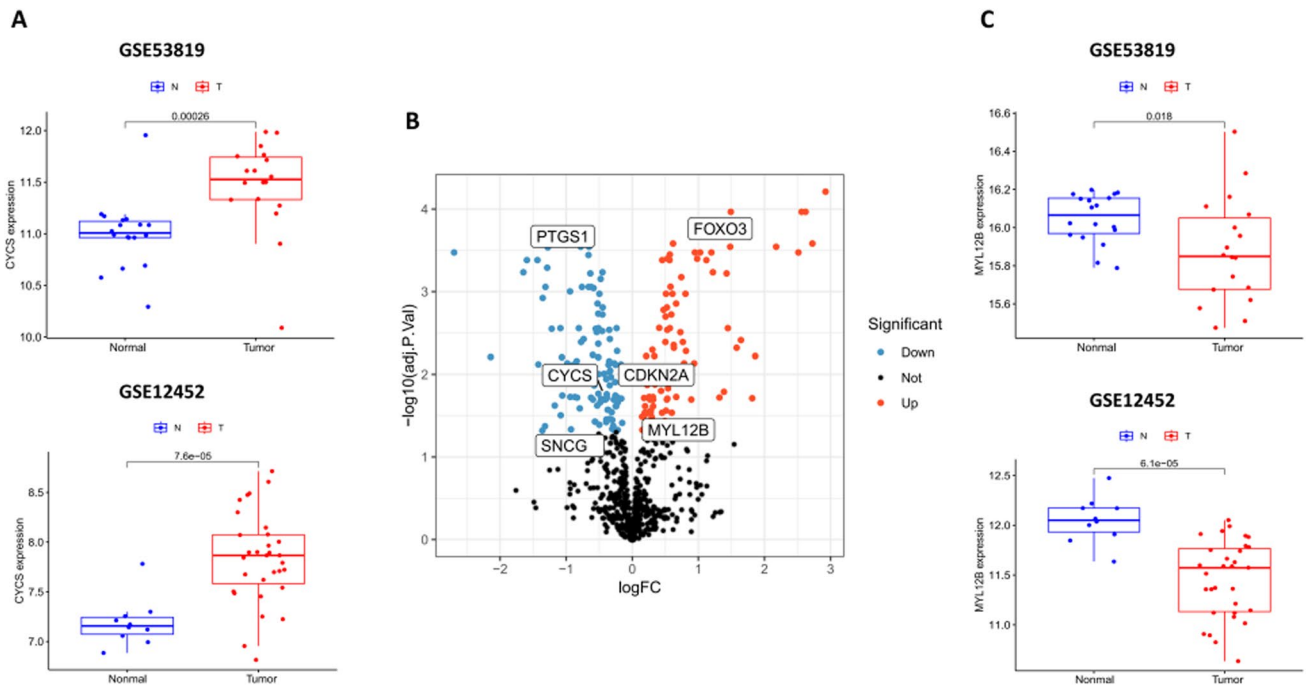

Fig. 7 To identify potential therapeutic targets for EGCG. **A** Expression of CYCS in the GEO cohort. **B** Visualized the distribution of the six-genes in the risk model within the previous volcano plot. **C** Expression of MYL12B in the GEO cohort

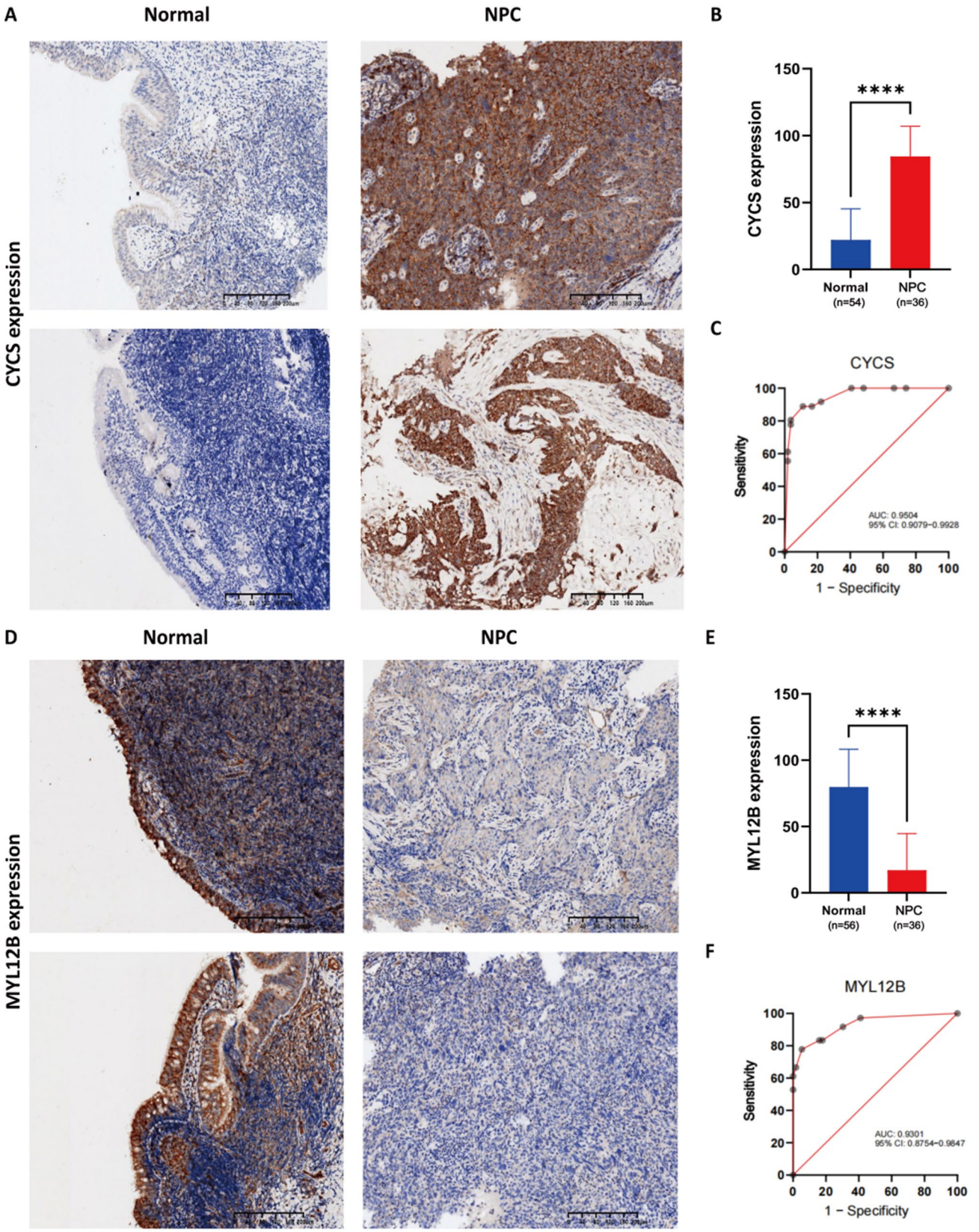

Fig. 8 Immunohistochemistry of CYCS, and MYL12B. **A**, **B** CYCS protein levels in NPC tissue expression. **C** Diagnostic efficacy of CYCS in NPC based on protein level. **D**, **E** MYL12B protein levels in NPC tissue expression. F Diagnostic efficacy of MYL12B in NPC based on protein level

Table 1 Binding energies of EGCG docking with 2 key target receptor protein molecules

Uniprot ID	Gene name	PDB ID	Binding energy (kcal/mol)
P99999	CYCS	2n3y	−7.9
O14950	MYL12B	AF-O14950-F1	−6

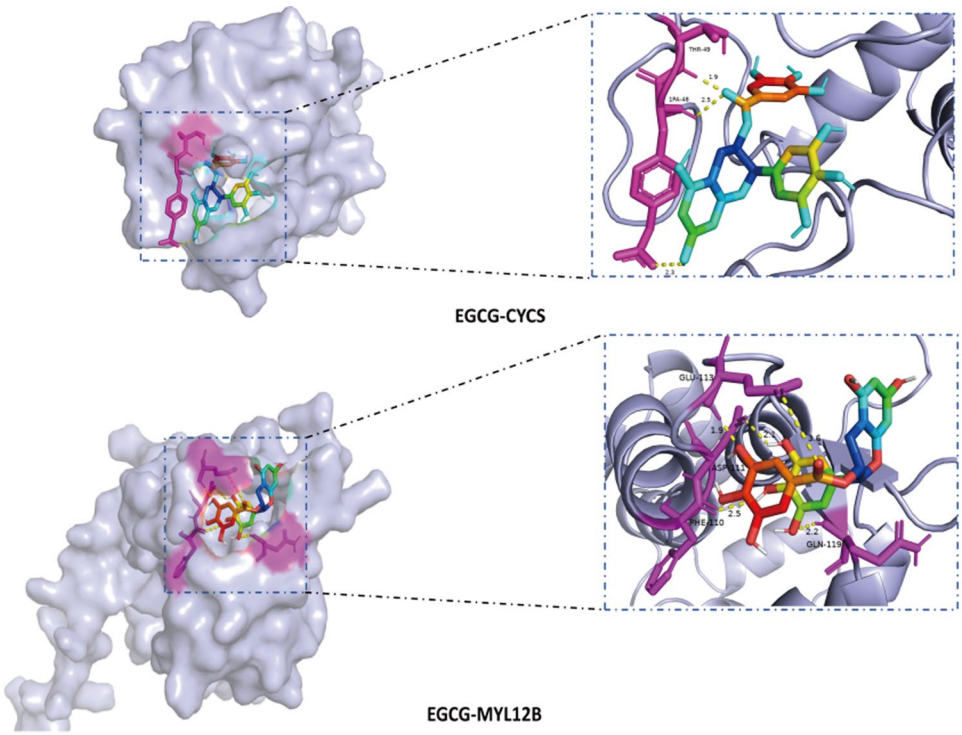

Fig. 9 Visualization of docking between EGCG and key targets molecules

PubChem (https://pubchem.ncbi.nlm.nih.gov). EGCG targets were also retrieved from TCMSP (https://old.tcmsp-e.com/tcmsp.php), SwissTargetPrediction (http://www.swisstargetprediction.ch) and TargetNet databases (http://targetnet.scbdd.com), following the probability criterion of > 0 in Swiss Target Prediction and Prob > 0 in TargetNet. After merging the results, duplicates were removed, and the UniProt protein database (https://www.uniprot.org) was used for standardising EGCG-related targets.

3.2 Data collection

mRNA expression profiles were obtained from the Gene Expression Omnibus (GEO) (https://www.ncbi.nlm.nih.gov/geo) for datasets GSE53819, GSE12452 and GSE102349, as outlined in Table 2. Selection criteria required control group sample sizes greater than 10 to minimise sampling errors and ensure reliable differential analysis. For the GSE102349 dataset, 88 of 113 patients had complete progression-free survival (PFS) data. No other publicly available datasets with prognostic information for NPC patients were identified, besides GSE102349. Additionally, a head and neck squamous cell carcinoma (HNSCC) dataset, containing 518 tissue samples with full clinical data from The Cancer Genome Atlas (TCGA), was used as a validation cohort.

Our approach to acquiring NPC cell lines is outlined as follows: Reagent preparation: EGCG was purchased from Sigma-Aldrich (St. Louis, USA). Master stock solutions were prepared in dimethyl sulfoxide (DMSO) and stored at −20°C. Working dilutions contained 0.1% v/v DMSO. Cell culture and treatment: HK1 cells were cultured as described previously [15]. Cells were seeded in 100 mm dishes (1.0×10^5 cells/well) and treated with EGCG (10 μg/ml, IC50 in HK1 cell line, data no shown) or DMSO (0.1% v/v) 24 h later. RNA was extracted from three independent experiments for sequencing.

Table 2 Basic information of GEO datasets in this study

GEO accession	Platform experiment type	Sample
GSE53819	GPL6480	Expression profiling by array 36 (18 normal + 18 NPC)
GSE12452	GPL570	Expression profiling by array 41 (10 normal + 31 NPC)
GSE102349	GPL11154	Expression profiling by high throughput sequencing 113 NPC

3.3 Identification of differentially expressed genes (DEGs) from HK1 NPC cell lines

DEGs associated with predicted EGCG targets were identified using the 'limma' package in R (version 4.3.2), comparing control and EGCG-treated groups. DEGs were defined using an adjusted P-value < 0.05. Visualisation of DEGs was performed using volcano plots and heatmaps, generated with the 'ggplot2' and 'pheatmap' packages in R.

3.4 Gene ontology (GO) and kyoto encyclopedia of genes and genomes (KEGG) analyses

In the present study, the R packages"clusterProfler"","org.Hs.eg.db"","enrichplot", and"ggplot2" (R version: 4.3.2) were utilized for the analysis of DEGs function. Additionally, a significance level of adjusted P < 0.05 was applied to filter the functional candidates.

3.5 Construction of a prognostic model based on the DEGs

These DEGs were analysed using univariate Cox regression, LASSO regression and multivariable Cox regression to construct a prognostic signature. The following computational formula was applied:

$$Risk\ score\ =\ \Sigma coef(gene)\ \times\ expr(gene)$$

The formula was utilized to calculate the risk score for each NPC patients. In all participating cohorts, samples were categorized into low-risk and high-risk groups based on the risk score (using median cut-off value). To assess the prognostic signature's impact on survival outcomes, an optimized cutoff and Kaplan–Meier (K-M) survival curve analysis were performed using R packages"survival" and"survminer". The predictive performance was evaluated through ROC curve analysis and risk plot presentation. Additionally, the accuracy of the risk score's predictions was further validated using the TCGA-HNSCC cohort.

3.6 Analysis of immune microenvironment

The immune, stromal, and ESTIMATE scores of NPC patients were obtained using the R package"ESTIMATE" [16]. To determine the proportion of immune-infiltrating cells in patients belonging to the high- and low-risk groups, single-sample gene set enrichment analysis (ssGSEA) was conducted using the R package"GSVA" [17]. The gene sets representing 24 [18] and 23 [19] types of immune cells used in this analysis were derived from existing literature.

3.7 The role of the predictive model in predicting the clinical treatment response

In order to assess the predictive model's role in determining the response to NPC treatment, we conducted an analysis of the half-maximal inhibitory concentration (IC50) of commonly used chemotherapy drugs for clinical NPC treatment. The Wilcoxon signed-rank test was employed to compare IC50 values between high- and low-risk groups.

3.8 Transcriptome differential analysis

R software (version 4.3.2) was used to analyse datasets GSE53819 and GSE12452, comparing prognostic gene expression between normal and tumour tissues. These results were then compared with those obtained from the NPC cell line analysis.

3.9 Immunohistochemistry staining assay

Paraffin-embedded tissue samples were obtained from 36 NPC patients and 24 individuals with normal nasopharyngeal epithelium. This study was approved by the Ethics Committee of the Affiliated Hospital of Guilin Medical University (No. 2024 WJWZCLL-29). Written informed consent was provided by all participants, including parents or legal guardians for subjects under the age of 16. Tissue sections with a thickness of 3 μm were prepared from the tissue samples. Subsequently, tissue sections underwent deparaffinization using xylene and were then subjected to antigen retrieval. The sections were further treated to block endogenous peroxidase activity by incubating them with 3% hydrogen peroxide for 15 min. Following this step, primary antibodies against CYCS (diluted 1:1000, #10,993–1-AP, Proteintech), and MYL12B (diluted 1:250, #10,324–1-AP, Proteintech) were applied, and the sections were left to incubate with the secondary antibody (kit-5020, MAIXIN BIOTECH, Fuzhou, China) for 70 min at room temperature. Following the immunostaining, the sections were developed using 3,3-diaminobenzidine reagent (DAB-1031, MAIXIN BIOTECH, Fuzhou, China) and counterstained with hematoxylin. The evaluation of immunostaining for each sample was conducted by two pathologists (Wenqi Luo and Xiaoyu Chen). Staining intensity was graded on a scale of 0 (absent), 1 (weak), 2 (moderate), or 3 (strong). The percentage of positive cells was scored as 0 (0%), 1 (1%–25%), 2 (26%–50%), 3 (51%–75%) or 4 (76%–100%). The final immunoreactivity score was determined by multiplying the staining intensity score by the percentage score, resulting in a scale from 0 to 12. Staining was evaluated under a pathological slice scanner (KF-PRO-020, KFBIO technology Inc, Zhejiang, China).

3.10 Molecular docking

Molecular docking analysis was employed to predict and evaluate the binding interactions and forces between proteins and small molecules. The molecular structure of EGCG was retrieved from the PubChem database (https://pubchem.ncbi.nlm.nih.gov) [20], while the protein structure was obtained from the PDB database (https://www.rcsb.org) [21]. To optimise the three-dimensional structure of EGCG, the MM2 force field was applied using the ChemBio3D Draw module in ChemBioOffice (version 2022). The structure was then converted into PDBQT format using Raccoon software [21]. For protein processing, MGLTools 1.5.7 (part of the Autodock Vina suite) was used to add hydrogen atoms and apply Gasteiger charges, which allowed for the merging of nonpolar hydrogen atoms [22]. The original PDB files were converted to the PDBQT format to ensure compatibility with Autodock Vina, providing the necessary ligand structures for molecular docking.

1. Ethics approval and consent to participate: This study was approved by the Ethics Committee of the Affiliated Hospital of Guilin Medical University (No.2024 WJWZCLL-29).
2. Accordance: This study was approved by the Ethics Committee of the Affiliated Hospital of Guilin Medical University (No. 2024 WJWZCLL-29).
3. Informed consent (for experiments involving humans or human tissue samples): Written informed consent was provided by all participants, including parents or legal guardians for subjects under the age of 16.

4 Discussion

Epidemiological studies have demonstrated an inverse association between the consumption of green tea and the incidence of certain cancers. Furthermore, long-term consumption of green tea may potentially reduce the risk of developing cancer and metastasis [23, 24]. Among these catechins, EGCG is the major component and exhibits various

biological activities including antibacterial, antiviral, cardiovascular protective, and antiangiogenic effects [6]. Currently, there is a growing global interest in the potential anti-cancer properties of EGCG. Research has indicated that EGCG may play a role in preventing and treating cancer by inhibiting cell proliferation, inducing apoptosis, interfering with cellular metabolism, suppressing oncogene expression, and inhibiting tumor neovascularization [25]. Moreover, EGCG has the potential to enhance the sensitivity of radioresistant cells by inhibiting Fatty Acid Synthase (FASN), positioning it as a promising candidate for development as a radiosensitizer aimed at improving treatment outcomes for NPC [8]. Therefore, EGCG warrants eval-uation and development as a therapeutic strategy in conjunction with radiotherapy to achieve more effective treatment for NPC patients.

In this study, we identified 198 DEGs. As previously noted, natural products have played a pivotal role in pharmacotherapy, particularly in cancer and infectious disease treatment [4, 5]. Among these, EGCG has been shown to confer various health benefits, including anti-tumour effects, antioxidant activity, anti-inflammatory properties, cardiovascular protection and neuroprotection [6, 7]. Our pathway analysis of the DEGs, enriched through KEGG, aligns well with previous studies. Consequently, we focused on pathways related to apoptosis, neurotrophic factor signalling and IL-17 signalling, all of which are relevant to cancer progression. Apoptosis, a conserved mechanism of programmed cell death, is a critical target in cancer treatment [26, 27]. Research has demonstrated that EGCG significantly inhibits cell proliferation and promotes apoptosis in NPC cell lines, including CNE-2 and 5-8 F [28]. Additionally, EGCG has been shown to inhibit proliferation, migration, invasion, spheroid formation and induce apoptosis in NPC cells in vitro, while reducing tumour growth in vivo [29]. Neurotrophins, typically known for supporting tumour development and progression, were also of interest in our study. The signalling pathways of NGF/TrkA, BDNF/TrkB and neurotrophins/p75 NTR have been linked to tumorigenesis [30]. In particular, the BDNF/TrkB pathway has been implicated in NPC, facilitating cellular migration and anoikis resistance [31]. The IL-17 signaling pathway plays a multifaceted role in the development of NPC, including promoting cell proliferation, migration, and invasion [32], as well as influencing tumor progression by regulating key signaling pathways and proinflammatory cytokine [33–35]. These findings provide potential targets for therapeutic strategies against the IL-17 signaling pathway in NPC [36].

GO analysis indicated that EGCG treatment of NPC is primarily associated with.

various biological processes, including responses to oxidative stress, cellular reactions to chemical stress, and the intrinsic apoptotic signaling pathway. Several studies have demonstrated that oxidative stress induces apoptosis in both normal nasopharyngeal epithelial cells and NPC cells; this process involves the activation of caspases, which can be inhibited by caspase inhibitors (CI) [37]. Furthermore, we found evidence suggesting that EGCG modulates apoptosis through the inhibition of the caspase protein family [38–40]. Therefore, the intervention of EGCG in NPC may be associated with the aforementioned biological processes, including oxidative stress and apoptosis.

To build a prognostic risk model, we conducted a systematic analysis of the DEGs, utilising both transcriptome data from GEO and clinical data. Through univariate Cox regression, LASSO regression analysis and multivariable Cox regression analysis, six genes were identified for inclusion in the model. Based on the calculated risk scores, patients were classified into high- and low-risk groups. The overall survival time in the high-risk group was significantly shorter than that in the low-risk group, and the ROC curve indicated that our model displayed strong predictive performance for NPC prognosis. These findings were further validated using the TCGA-HNSCC cohort, where a similar trend in survival outcomes was observed.

The risk model consists of six genes: SNCG, FOXO3, PTGS1, CDKN2 A, MYL12B, and CYCS, all of which are associated with the prognosis of NPC.

SNCG, also referred to as γ-synuclein and breast cancer-specific gene 1 (BCSG1), is a member of the synuclein family, alongside SNCA and SNCB [41]. Research has shown that the mechanism by which EGCG modulates γ-synuclein fibrillation provides valuable insights for the treatment of synucleopathies [42]. Forkhead box O3 (FOXO3), formerly referred to as FOXO3a and FKHR-L1, is a member of the class 'O' subfamily of Forkhead box proteins (FOXOs) [43, 44]. We have identified FOXO transcription factors as critical cellular targets for anti-tumor drugs across different cancer types such as breast cancer [45–47], chronic myeloid leukemia [48, 49], and colon cancer [50]. Prostaglandin endoperoxidase (PTGS), also known as cyclooxygenase (COX), is a crucial enzyme involved in the biosynthesis of prostaglandins [51]. Cyclin-dependent kinase inhibitor 2 A (CDKN2 A), also known as p16, is a critical tumour suppressor protein that prevents inappropriate cell proliferation. Studies suggest that CDKN2 A/p16 may serve as an independent biomarker for predicting treatment response in NPC. Researchers observed improved PFS and locoregional control (LRC) in patients with CDKN2 A/p16-positive tumours, regardless of EBV status [52]. This finding aligns with our univariate and multivariable Cox regression analyses. Additionally, multiple studies have explored the role of EGCG in evading anti-growth signalling pathways [53]. The loss or dysfunction of tumour suppressor genes like CDKN2 A is

common in solid tumours, leading to the unregulated activation of tumour growth-promoting pathways [54]. EGCG has shown promise in disrupting this signalling pathway [55]. Myosin II is an actin-binding protein composed of myosin heavy chains (MHC IIs), regulatory light chains (RLCs), and essential light chains (ELCs). In non-muscle cells, the activity of myosin II is regulated by RLCs, which include three highly conserved non-muscle RLC isoforms: MYL12 A, MYL12B, and MYL9 [56]. Meanwhile, MYL12B was identified for the first time as prognostic signature genes for NPC in this study. CYCS is a key component of the mitochondrial electron transport chain, primarily responsible for energy production in both normal and cancerous cells [57]. Mutations in CYCS can trigger apoptosis in oral squamous cell carcinoma cells [58]. Setareh Shojaei et al. [59] also reported that CYCS upregulation is strongly associated with poor prognosis in HNSCC. Our study similarly revealed that CYCS is highly expressed in NPC cases and correlates with unfavourable PFS outcomes, consistent with prior research.

In currently, novel chemotherapy drugs have become a hot topic of research, sig-nificantly enhancing the sensitivity of NPC cells to chemotherapeutic agents and radiotherapy [60–64], thereby reducing related complications [65]. These drugs primarily exert their effects through several mechanisms: Firstly, by blocking the cell cycle to inhibit cell proliferation [66] [67]. Secondly, some drugs can suppress epithelial-mesenchymal transition (EMT) to curb the metastatic and invasive capa-bilities [68]. Lastly, certain drugs can block immune evasion and enhance immune responses [60]. This study revealed significant differences among these drugs in the constructed models through drug sensitivity analysis. With a deeper understanding of the mechanisms of action of these drugs, we hope to develop more effective treatment plans to improve the prognosis and quality of life for patients with NPC.

In the progression of tumors, the immune components of the tumor microenviron-ment play a pivotal role and have become a hot topic in research. In this study, we found significant differences in the distribution of five immune subpopulations between the high-risk and low-risk groups. Additionally, a research team has discovered that NK cells in NPC tissue act as an independent prognostic factor closely related to tumor recurrence and metastasis [69]. Another study on HNSCC also found that high infiltration of Treg cells in the tissue is positively correlated with a favorable progno-sis in patients [70]. These research findings are consistent with our discoveries, further supporting our hypothesis that the model may play a key role by modulating the immune components of the tumor microenvironment in patients with NPC.

In addition, differential expression analysis from two GEO datasets indicated that CYCS was highly expressed, while MYL12B was expressed at lower levels in NPC tissues. These findings were further validated by IHC experiments using clinical tissue samples. However, this result contradicts the differential expression analysis conducted on NPC cell lines, which showed downregulation of CYCS and upregulation of MYL12B. This discrepancy may be attributed to EGCG's ability to downregulate CYCS and upregulate MYL12B. Therefore, we speculate that these two genes could serve as potential targets for EGCG treatment.

Nevertheless, this study has several limitations. The data were derived from the GEO database, which may be influenced by experimental conditions, sample characteristics and potential confounding factors. Furthermore, the TCGA-HNSCC dataset used for model validation is broad and lacks the necessary specificity for NPC. The relatively small sample size for the IHC experiments may also introduce potential inaccuracies. Thus, while our research highlights the potential predictive value of this risk model in NPC, further validation through prospective studies is required to confirm these findings and ensure reliable outcomes.

5 Conclusions

We collaboratively developed a prognostic risk model based on EGCG targeting and NPC, and identified two pivotal target genes: CYCS and MYL12B. This model holds promise for guiding future NPC-targeted therapeutic strategies. However, our study still has limitations, for instance, we did not conduct in vitro and in vivo experiments to verify the capabilities of relevant targets. The journey towards clinical application of EGCG-related targets in NPC treatment remains lengthy. The depth of pharmacological research in this area is insufficient, warranting further interdisciplinary exploration. Additionally, more extensive animal studies are imperative to assess potential safety and efficacy metrics.

Acknowledgements We acknowledge TCGA and GEO database for providing their platforms and contributors for uploading their meaningful datasets. We thank Bullet Edits Limited for the linguistic editing and proofreading of the manuscript.

Author contributions Yuhang Yang and Wenqi Luo contributed equally to the article. (I) Conception and design: Y Yang, W Luo; (II) Administrative support: F He, F Liu;:: (III) Provision of study materials or patients: W Wang, X Cheng, W Luo, X He, Z Feng;:: (IV) Collection and assembly of

data: L Zuo, M Duan and J Li; (V) Data analysis and interpretation: Y Yang; (VI) Manuscript writing: all authors; (VII) Final approval of manuscript: all authors.

Funding This work was supported by the Natural Science Foundation of guangxi Province, China (No. 2022GXNSFBA035507).

Data availability This study was approved by the Ethics Committee of the Affiliated Hospital of Guilin Medical University (No. 2024 WJWZ-CLL-29). Written informed consent was provided by all participants, including parents or legal guardians for subjects under the age of 16. All experiments were performed in accordance with relevant guidelines and regulations. Data is provided within the supplementary information files.

Declarations

Ethics approval and consent to participate: This study was approved by the Ethics Committee of the Affiliated Hospital of Guilin Medical University (No. 2024 WJWZCLL-29). Written informed consent was provided by all participants, including parents or legal guardians for subjects under the age of 16. All experiments were performed in accordance with relevant guidelines and regulations.

Consent for publication Not applicable.

Competing interests The authors declare no competing interests.

References

1. Chen Y-P, Chan AT, Le Q-T, Blanchard P, Sun Y, Ma J. Nasopharyn-geal carcinoma. Lancet. 2019;394(10192):64–80.
2. Lee HM, Okuda KS, Gonzalez FE, Patel V. Current perspectives on nasopharyngeal carcinoma. Human Cell Transform. 2019;1:11–34.
3. Ke L-R, Xia W-X, Qiu W-Z, Huang X-J, Yu Y-H, Liang H, Liu G-Y, Xiang Y-Q, Guo X, Lv X. A phase ii trial of induction nab-paclitaxel and cisplatin followed by concurrent chemoradiotherapy in patients with locally advanced nasopharyngeal carcinoma. Oral Oncol. 2017;70:7–13.
4. Sibley CH. Understanding artemisinin resistance. Science. 2015;347(6220):373–4.
5. Romano A, Martel F. The role of egcg in breast cancer prevention and therapy. Mini Rev Med Chem. 2021;21(7):883–98.
6. Chakrawarti L, Agrawal R, Dang S, Gupta S, Gabrani R. Therapeutic effects of egcg: a patent review. Expert Opin Ther Pat. 2016;26(8):907–16.
7. Negri A, Naponelli V, Rizzi F, Bettuzzi S. Molecular targets of epigallocate-chin—gallate (egcg): A special focus on signal transduction and cancer. Nutrients. 2018;10(12):1936.
8. Chen J, Zhang F, Ren X, Wang Y, Huang W, Zhang J, Cui Y. Targeting fatty acid synthase sensitizes human nasopharyngeal carcinoma cells to radiation via downregulating frizzled class receptor 10. Cancer Biol Med. 2020;17(3):740.
9. Xing L, Guo M, Zhang X, Zhang X, Liu F. A transcriptional metabolic gene-set based prognostic signature is associated with clinical and mutational features in head and neck squamous cell carcinoma. J Cancer Res Clin Oncol. 2020;146:621–30.
10. He L, Chen J, Xu F, Li J. Prognostic implication of a metabolism-associated gene signature in lung adenocarcinoma. Mol Ther. 2020;19:265–77.
11. Cheong J-H, Wang SC, Park S, Porembka MR, Christie AL, Kim H, Kim HS, Zhu H, Hyung WJ, Noh SH, et al. Development and valida-tion of a prognostic and predictive 32-gene signature for gastric cancer. Nat Commun. 2022;13(1):774.
12. Zhu Q, Rao B, Chen Y, Jia P, Wang X, Zhang B, Wang L, Zhao W, Hu C, Tang M, et al. In silico development and in vitro validation of a novel five-gene signature for prognostic prediction in colon cancer. Am J Cancer Res. 2023;13(1):45.
13. Su M, Guo C, Liu M, Liang X, Yang B. Therapeutic targets of vita-min c on liver injury and associated biological mechanisms: a study of network pharmacology. Int Immunopharmacol. 2019;66:383–7.
14. Wishart DS, Feunang YD, Guo AC, Lo EJ, Marcu A, Grant JR, Sajed T, Johnson D, Li C, Sayeeda Z, et al. Drugbank 5.0: a major update to the drugbank database for 2018. Nucleic Acids Res. 2018;46(11):1074–82.
15. He F, Feng G, Ma N, Midorikawa K, Oikawa S, Kobayashi H, Zhang Z, Huang G, Takeuchi K, Murata M. Gdf10 inhibits cell proliferation and epithelial–mesenchymal transition in nasopharyngeal carcinoma by the trans-forming growth factor-β/smad and nf-κb pathways. Carcinogenesis. 2022;43(2):94–103.
16. Yoshihara K, Shahmoradgoli M, Martınez E, Vegesna R, Kim H, Torres-Garcia W, Trevino V, Shen H, Laird PW, Levine DA, et al. Inferring tumour purity and stromal and immune cell admixture from expression data. Nat Commun. 2013;4(1):2612.
17. Hanzelmann S, Castelo R, Guinney J. Gsva: gene set variation analysis for microarray and rna-seq data. BMC Bioinform. 2013;14:1–15.
18. Bindea G, Mlecnik B, Tosolini M, Kirilovsky A, Waldner M, Obenauf AC, Angell H, Fredriksen T, Lafontaine L, Berger A, et al. Spatiotemporal dynamics of intratumoral immune cells reveal the immune landscape in human cancer. Immunity. 2013;39(4):782–95.

19. Charoentong P, Finotello F, Angelova M, Mayer C, Efremova M, Rieder D, Hackl H, Trajanoski Z. Pan-cancer immunogenomic analyses reveal genotype-immunophenotype relationships and predictors of response to check-point blockade. Cell Rep. 2017;18(1):248–62.
20. Wang Y, Bryant SH, Cheng T, Wang J, Gindulyte A, Shoemaker BA, Thiessen PA, He S, Zhang J. Pubchem bioassay: 2017 update. Nucleic Acids Res. 2017;45(D1):955–63.
21. Burley SK, Berman HM, Kleywegt GJ, Markley JL, Nakamura H, Velankar S. Protein data bank (pdb): the single global macromolecular structure archive. Protein Crystallogr. 2017;1:627–41.
22. Trott O, Olson AJ. Autodock vina: improving the speed and accuracy of docking with a new scoring function, efficient optimization, and multithreading. J Comput Chem. 2010;31(2):455–61.
23. Yang CS, Wang X, Lu G, Picinich SC. Cancer prevention by tea: animal studies, molecular mechanisms and human relevance. Nat Rev Cancer. 2009;9(6):429–39.
24. Trudel D, Labbe DP, Bairati I, Fradet V, Bazinet L, Tetu B. Green tea for ovarian cancer prevention and treatment: a systematic review of the in vitro, in vivo and epidemiological studies. Gynecol Oncol. 2012;126(3):491–8.
25. Wang Y-Q, Lu J-L, Liang Y-R, Li Q-S. Suppressive effects of egcg on cervical cancer. Molecules. 2018;23(9):2334.
26. Carneiro BA, El-Deiry WS. Targeting apoptosis in cancer therapy. Nat Rev Clin Oncol. 2020;17(7):395–417.
27. Liu X, Jiang Q, Liu H, Luo S. Vitexin induces apoptosis through mitochon-drial pathway and pi3k/akt/mtor signaling in human non-small cell lung cancer a549 cells. Biol Res. 2019;52:1–7.
28. Jiang S, Huang C, Zheng G, Yi W, Wu B, Tang J, Liu X, Huang B, Wu D, Yan T, et al. Egcg inhibits proliferation and induces apoptosis through downregulation of sirt1 in nasopharyngeal carcinoma cells. Front Nutr. 2022;9: 851972.
29. Fang C-Y, Wu C-C, Hsu H-Y, Chuang H-Y, Huang S-Y, Tsai C-H, Chang Y, Tsao GS-W, Chen C-L, Chen J-Y. Egcg inhibits proliferation, invasiveness and tumor growth by up-regulation of adhesion molecules, suppression of gelatinases activity, and induction of apoptosis in nasopharyngeal carcinoma cells. Int J Mol Sci. 2015;16(2):2530–58.
30. Chopin V, Lagadec C, Toillon R-A, Le Bourhis X. Neurotrophin signaling in cancer stem cells. Cell Mol Life Sci. 2016;73(9):1859–70.
31. Ng Y-K, Wong EYL, Lau CPY, Chan JPL, Wong SCC, Chan AS-K, Kwan MPC, Tsao S-W, Tsang C-M, Lai PBS, et al. K252a induces anoikis-sensitization with suppression of cellular migration in epstein-barr virus (ebv)—associated nasopharyngeal carcinoma cells. Invest New Drugs. 2012;30:48–58.
32. Zou Z, Gan S, Liu S, Li R, Huang J. Investigation of differentially expressed genes in nasopharyngeal carcinoma by integrated bioinformatics analysis. Oncol Lett. 2019;18(1):916–26.
33. Wu D, Wang J, Pae M, Meydani SN. Green tea egcg, t cells, and t cell-mediated autoimmune diseases. Mol Aspects Med. 2012;33(1):107–18.
34. Wang J, Ren Z, Xu Y, Xiao S, Meydani SN, Wu D. Epigallocatechin-3-gallate ameliorates experimental autoimmune encephalomyelitis by altering balance among cd4+ t-cell subsets. Am J Pathol. 2012;180(1):221–34.
35. Min S-Y, Yan M, Kim SB, Ravikumar S, Kwon S-R, Vanarsa K, Kim H-Y, Davis LS, Mohan C. Green tea epigallocatechin-3-gallate suppresses autoimmune arthritis through indoleamine-2, 3-dioxygenase expressing dendritic cells and the nuclear factor, erythroid 2-like 2 antioxidant pathway. J Inflamm. 2015;12:1–15.
36. Wang L, Ma R, Kang Z, Zhang Y, Ding H, Guo W, Gao Q, Xu M. Effect of il-17a on the migration and invasion of npc cells and related mechanisms. PLoS ONE. 2014;9(9): 108060.
37. Tan S-N, Sim S-P, Khoo AS. Potential role of oxidative stress-induced apoptosis in mediating chromosomal rearrangements in nasopharyngeal carcinoma. Cell Biosci. 2016;6:1–16.
38. Bao B, Yin X-P, Wen X-Q, Suo Y-J, Chen Z-Y, Li D-L, Lai Q, Cao X-M, Qu Q-M. The protective effects of egcg was associated with ho-1 active and microglia pyroptosis inhibition in experimental intracerebral hemorrhage. Neurochem Int. 2023;170: 105603.
39. He Q, Bao L, Zimering J, Zan K, Zhang Z, Shi H, Zu J, Yang X, Hua F, Ye X, et al. The protective role of (-)-epigallocatechin-3-gallate in thrombin-induced neuronal cell apoptosis and jnk-mapk activation. NeuroReport. 2015;26(7):416–23.
40. Yun M, Seo G, Lee J-Y, Chae GT, Lee S-B. Epigallocatechin-3-gallate attenuates the aim2-induced secretion of il-1β in human epidermal keratinocytes. Biochem Biophys Res Commun. 2015;467(4):723–9.
41. Liu C, Qu L, Shou C. Role and characterization of synuclein-γ unconventional protein secretion in cancer cells. Unconvent Prot Secr. 2016;1:215–27.
42. Roy S, Bhat R. Suppression, disaggregation, and modulation of γ-synuclein fibrillation pathway by green tea polyphenol egcg. Protein Sci. 2019;28(2):382–402.
43. Yusuf D, Butland SL, Swanson MI, Bolotin E, Ticoll A, Cheung WA, Cindy Zhang XY, Dickman CT, Fulton DL, Lim JS, et al. The transcription factor encyclopedia. Genome Biol. 2012;13:1–25.
44. Chiacchiera F, Simone C. The ampk-foxo3a axis as a target for cancer treatment. Cell Cycle. 2010;9(6):1091–6.
45. Sunters A, Mattos SF, Stahl M, Brosens JJ, Zoumpoulidou G, Saunders CA, Coffer PJ, Medema RH, Coombes RC, Lam EW-F. Foxo3a transcriptional regulation of bim controls apoptosis in paclitaxel-treated breast cancer cell lines. J Biol Chem. 2003;278(50):49795–805.
46. Sunters A, Madureira PA, Pomeranz KM, Aubert M, Brosens JJ, Cook SJ, Burgering BM, Coombes RC, Lam EW-F. Paclitaxel-induced nuclear translocation of foxo3a in breast cancer cells is mediated by c-jun nh2-terminal kinase and akt. Can Res. 2006;66(1):212–20.
47. Krol J, Francis RE, Albergaria A, Sunters A, Polychronis A, Coombes RC, Lam EW-F. The transcription factor foxo3a is a crucial cellular target of gefitinib (iressa) in breast cancer cells. Mol Cancer Ther. 2007;6(12):3169–79.
48. Mattos SF, Essafi A, Soeiro I, Pietersen AM, Birkenkamp KU, Edwards CS, Martino A, Nelson BH, Francis JM, Jones MC, et al. Foxo3a and bcr-abl regulate cyclin d2 transcription through a stat5/bcl6-dependent mechanism. Mol Cell Biol. 2004;1:1.
49. Essafi A, Mattos S, Hassen YA, Soeiro I, Mufti GJ, Thomas NSB, Medema RH, Lam EW. Direct transcriptional regulation of bim by foxo3a mediates sti571-induced apoptosis in bcr-abl-expressing cells. Oncogene. 2005;24(14):2317–29.
50. Mattos S, Villalonga P, Clardy J, Lam EW. Foxo3a mediates the cytotoxic effects of cisplatin in colon cancer cells. Mol Cancer Ther. 2008;7(10):3237–46.
51. Cebola I, Custodio J, Munoz M, Dıez-Villanueva A, Pare L, Prieto P, Ausso S, Coll-Mulet L, Bosca L, Moreno V, et al. Epigenetics override pro-inflammatory ptgs transcriptomic signature towards selective hyperactivation of pge 2 in colorectal cancer. Clin Epigen. 2015;7:1–11.

52. Shimizu Y, Murakami N, Mori T, Takahashi K, Kubo Y, Yoshimoto S, Honma Y, Nakamura S, Okamoto H, Iijima K, et al. Clinical impact of p16 positivity in nasopharyngeal carcinoma. Laryngosc Invest Otolaryngol. 2022;7(4):994–1001.
53. Talib WH, Awajan D, Alqudah A, Alsawwaf R, Althunibat R, Abu AlRoos M, Al Safadi A, Abu Asab S, Hadi RW, Al Kury LT, et al. Targeting cancer hallmarks with epigallocatechin gallate (egcg): mechanistic basis and therapeutic targets. Molecules. 2024;29(6):1373.
54. Lin LL, Choucair K, Patel R. Nf1 in solid tumors: The unknown soldier of tumor suppressor genes. Genet Mol Med. 2019;1(1):1–13.
55. Sharifi-Rad M, Pezzani R, Redaelli M, Zorzan M, Imran M, Ahmed Khalil A, Salehi B, Sharopov F, Cho WC, Sharifi-Rad J. Preclinical activities of epigallocatechin gallate in signaling pathways in cancer. Molecules. 2020;25(3):467.
56. Park I, Han C, Jin S, Lee B, Choi H, Kwon JT, Kim D, Kim J, Lifirsu E, Park WJ, et al. Myosin regulatory light chains are required to maintain the stability of myosin ii and cellular integrity. Biochem J. 2011;434(1):171–80.
57. Huttemann M, Pecina P, Rainbolt M, Sanderson TH, Kagan VE, Sama-vati L, Doan JW, Lee I. The multiple functions of cytochrome c and their regulation in life and death decisions of the mammalian cell: from respiration to apoptosis. Mitochondrion. 2011;11(3):369–81.
58. Sabit H, Tombuloglu H, Cevik E, Abdel-Ghany S, El-Zawahri E, El-Sawy A, Isik S, Al-Suhaimi E. Knockdown of c-myc controls the proliferation of oral squamous cell carcinoma cells in vitro via dynamic regulation of key apoptotic marker genes. Int J Mol Cell Med. 2021;10(1):45.
59. Shojaei S, Menbari P, Jamshidi S, Taherkhani A. Microrna-based markers of oral tongue squamous cell carcinoma and buccal squamous cell carcinoma: a systems biology approach. Biochem Res Int. 2023;2023(1):5512894.
60. Liang L, Yue C, Li W, Tang J, He Q, Zeng F, Cao J, Liu S, Chen Y, Li X, et al. Cd38 symmetric dimethyl site r58 promotes malignant tumor cell immune escape by regulating the camp-gsk3β-pd-l1 axis. Heliyon. 2024;10:19.
61. Lu Q-P, Chen W-D, Peng J-R, Xu Y-D, Cai Q, Feng G-K, Ding K, Zhu X-F, Guan Z. Antitumor activity of 7rh, a discoidin domain receptor 1 inhibitor, alone or in combination with dasatinib exhibits antitumor effects in nasopharyngeal carcinoma cells. Oncol Lett. 2016;12(5):3598–608.
62. Shi L, Mei Y, Duan X, Wang B. [retracted] effects of cisplatin combined with metformin on proliferation and apoptosis of nasopharyngeal carcinoma cells. Comput Math Methods Med. 2022;2022(1):2056247.
63. Chong WQ, Lim CM, Sinha AK, Tan CS, Chan GHJ, Huang Y, Kumarakulasinghe NB, Sundar R, Jeyasekharan AD, Loh WS, et al. Integration of antiangiogenic therapy with cisplatin and gemcitabine chemotherapy in patients with nasopharyngeal carcinoma. Clin Cancer Res. 2020;26(20):5320–8.
64. Zhang S, Lin S, Hu L. Lobaplatin combined with docetaxel neoadjuvant chemotherapy followed by concurrent lobaplatin with intensity-modulated radiotherapy increases the survival of patients with high-risk lymph node positive nasopharyngeal carcinoma. J buon. 2016;21(1):161–7.
65. Sun X, Zhu Y, Lou Y, Lu X, Wang B, Yu D, Guo Y, Xin Y. Anti-angiogenesis agents plus chemoradiotherapy for locally advanced nasopharyngeal cancer: a systematic review and meta-analysis. Eur Arch Oto-Rhino-Laryngol. 2024;1:1–13.
66. Zhao L, Wen Z-H, Jia C-H, Li M, Luo S-Q, Bai X-C. Metformininduces g1 cell cycle arrest and inhibits cell proliferation in nasopharyngeal carcinoma cells. Anat Rec Adv Integr Anat Evol Biol. 2011;294(8):1337–43.
67. Hui EP, Lui VW, Wong CS, Ma BB, Lau CP, Cheung CS, Ho K, Cheng S-H, Ng MH, Chan AT. Preclinical evaluation of sunitinib as single agent or in combination with chemotherapy in nasopharyngeal carcinoma. Invest New Drugs. 2011;29:1123–31.
68. Li Y-J, He Y-F, Han X-H, Hu B. Dasatinib suppresses invasion and induces apoptosis in nasopharyngeal carcinoma. Int J Clin Exp Pathol. 2015;8(7):7818.
69. Li Y, Dong H, Dong Y, Wu Q, Jiang N, Luo Q, Chen F. Distribution of cd8 t cells and nk cells in the stroma in relation to recurrence or metastasis of nasopharyngeal carcinoma. Cancer Manag Res. 2022;1:2913–26.
70. Bron L, Jandus C, Andrejevic-Blant S, Speiser DE, Monnier P, Romero P, Rivals J-P. Prognostic value of arginase-ii expression and regulatory t-cell infiltration in head and neck squamous cell carcinoma. Int J Cancer. 2013;132(3):85–93.